

Cite this: DOI: 10.1039/c0xx00000x

www.rsc.org/xxxxxx

ARTICLE TYPE

## Gallium(III) complexes of NOTA-bis(phosphonate) conjugates as PET radiotracers for bone imaging

Jan Holub,<sup>a</sup> Marian Meckel,<sup>b</sup> Vojtěch Kubiček,<sup>a</sup> Frank Rösch<sup>b</sup> and Petr Hermann<sup>\*a</sup>

Received (in XXX, XXX) Xth XXXXXXXXX 20XX, Accepted Xth XXXXXXXXX 20XX

DOI: 10.1039/b000000x

Bone-targeting geminal bis(phosphonic acid) moiety, as a distant non-coordinating group, was appended to the 1,4,7-triazacyclonone-1,4-diacetic acid fragment through acetamide (NOTAM<sup>BP</sup>) or methylenephosphinate (NO2AP<sup>BP</sup>) spacers bound to the last ring nitrogen atom. The macrocycles were investigated as ligands for potential <sup>68</sup>Ga-PET bone imaging radiopharmaceuticals. Complexation of Ga(III) proceeds through *out-of-cage* intermediates with coordinated bis(phosphonate) group to final species with Ga(III) ion inside the macrocyclic cavity. Rate of formation of the final *in-cage* complex is strongly dependent on the nature of the spacer connecting the bis(phosphonate) group to the macrocycle. Much faster complexation was observed for the methylenephosphinate spacer if compared with that for the acetamide one. This trend was also observed during radiolabeling studies with no-carrier-added <sup>68</sup>Ga. For both ligands, formation of the Ga(III) complex was slower than that with NOTA due to strong binding of the bis(phosphonate) group in the intermediate *out-of-cage* complex. Complexation was efficient and fast only above 60 °C and in a rather narrow acidity region (around pH 3). Hydrolysis of the amide bond of the carboxamide-bis(phosphonate) conjugate was observed during complexation reaction leading to the Ga-NOTA complex. However, ligand degradation proceeds slowly even at high temperature and, thus, was negligible during radiolabeling. *In vitro* sorption studies confirmed effective binding of the <sup>68</sup>Ga complexes to hydroxyapatite being comparable with that for common bis(phosphonate) drugs such as pamidronate. Selective bone uptake was confirmed by biodistribution studies *ex vivo* and microPET imaging in healthy rats *in vivo*. Bone uptake was very high (4.37±0.92 % ID/g for [<sup>68</sup>Ga]NO2AP<sup>BP</sup>) at 60 min p.i., which is superior to the uptake of <sup>68</sup>Ga-DOTA-based bis(phosphonates) reported earlier (2.58±0.33 % ID/g for [<sup>68</sup>Ga]DO3AP<sup>BP</sup> at 60 min p.i.). Coincidentally, accumulation in soft tissue is general low (e.g. for kidneys 0.18±0.7 % ID/g for [<sup>68</sup>Ga]NO2AP<sup>BP</sup> at 60 min p.i.), revealing the new <sup>68</sup>Ga complexes as ideal tracers for non-invasive, fast and quantitative imaging of calcified tissue and for metastatic lesions using PET or PET/CT.

### Introduction

Positron emission tomography (PET) is a powerful method for imaging various tissue or physiological states. The choice of the proper PET radionuclide is given by various criteria such as half-life, energy of the emitted positron, production pathway, radiopharmaceuticals preparation, means of application etc. Compared to the most commonly used radioisotopes (<sup>11</sup>C and <sup>18</sup>F) needing on-site production on a cyclotron, various metal radionuclides can conveniently be prepared utilizing a generator – a device containing a parent nuclide that decays with a long half-time to a daughter positron-emitting radionuclide which is periodically eluted off, purified and used. These radionuclide generators are relatively cheap, permanently accessible and easy to handle. One of the most promising generator-produced radionuclides is <sup>68</sup>Ga (*t*<sub>1/2</sub> 67.7 min, 89 % positron emission, mean  $\gamma$  energy 0.83 MeV)<sup>1</sup> available from commercial <sup>68</sup>Ge/<sup>68</sup>Ga generators.

However, with only very limited exceptions, most of the metal radioisotopes cannot be applied in a “free” form. The metal radioisotope must be bound in a stable complex to avoid non-specific deposition of the radioisotope in tissues. Ligands used for complexation of the metal ions must ensure very fast and efficient complexation even in highly diluted solutions, sufficient kinetic inertness and thermodynamic stability of the complexes as well as specific accumulation of the formed species in the tissue of interest. The last requirement is commonly fulfilled either by creating a metal-ligand system showing specific interaction with target organs or by adding a biologically relevant targeting vector to the metal-ligand system, thereby turning the “normal” ligand into a “bifunctional” one. Bifunctionality defines the utilization of one of the functional groups of the ligand to covalent attachment of the ligand to the targeting vector while preserving the complexing potency of the remaining structure.

Bone tissue is a prominent target of radionuclide diagnostics and therapeutics as bone metastases represent a very common complication of various types of cancer. Generally, bone

targeting is mostly realized via attachment of a geminal bis(phosphonate) moiety to a molecule to be delivered to bone.<sup>2,3,4</sup> [5] Bis(phosphonates) show a high affinity to hydroxyapatite (HAP). Thus, compounds containing a bis(phosphonate) moiety are efficiently adsorbed on the surface of bones. Consequently, such conjugates have been used to deliver radioisotopes to the calcified tissues.<sup>4</sup> Recently, we and others have developed bis(phosphonate)-bearing ligands based on a DOTA-like macrocyclic core (Figure 1) as carriers for metal ions to be delivered to calcified tissue.<sup>[6,7,8,9,10,11]</sup> The applications include imaging techniques (<sup>111</sup>In/<sup>177</sup>Lu and <sup>68</sup>Ga for SPECT and PET imaging, respectively)<sup>[7,9,11,12,13]</sup> as well as therapy (<sup>177</sup>Lu, <sup>90</sup>Y)<sup>7,10</sup> or bone metastases pain palliation in human patients.<sup>14</sup> The conjugates exhibited a very high affinity to HAP as the bis(phosphonate) moiety is not coordinated to the central metal ion and, thus, remains active for bone targeting.<sup>15,16</sup> However, DOTA-like macrocycles are not the best ligands for Ga(III) as incorporation of the ion inside the macrocyclic cavity leads to severe distortion of coordination octahedron around Ga(III) ion.<sup>17</sup> Despite high thermodynamic stability and kinetic inertness of the Ga(III) complexes with DOTA-like ligands,<sup>18</sup> complexation of no-carrier-added (NCA) <sup>68</sup>Ga with these ligands is less efficient and more sensitive to experimental conditions than that of NOTA analogs (Figure 1).<sup>1</sup> Triaza- instead of tetraazacycles have been proved to be more suitable for Ga(III). They form complexes exhibiting much higher thermodynamic stability as well as kinetic inertness.<sup>[19,20]</sup>

The size of the coordination cavity imposed by the nine-member macrocyclic ring corresponds very well to the size of the Ga(III) ion. In addition, the ligands provide just six donor groups perfectly matching Ga(III) requirements for the octahedral coordination sphere ( $\log K_{[\text{Ga-DOTA}]} = 26.1$ ,<sup>18</sup>  $\log K_{[\text{Ga-NOTA}]} = 29.6$ <sup>19</sup>). Thus, a number of NOTA-like ligands have been investigated as promising chelators for <sup>68</sup>Ga.<sup>1,4</sup> Among them (by analogy with the most commonly used ligands in the DOTA-like family, the DOTA-monoamides), NOTA-monoamides appear as an emerging class of ligands due to their easy synthesis and potential easiness of introduction of bifunctionality through amide formation.<sup>21,22</sup>

Thus, in order to improve properties of the bone-targeted complexes such as ease of labeling and improved bone/soft tissue ratio, the NOTA-like macrocyclic skeleton (as the efficient <sup>68</sup>Ga-binding motif) is combined with a distant bis(phosphonate)-containing side arm (as the bone-targeting group) through the methylphosphinate or acetamide pendant arms as spacers resulting in new ligands, NOTAM<sup>BP</sup> and NO2AP<sup>BP</sup> (Figure 1). In order to simplify the text, abbreviations as NOTA, Ga-NOTAM<sup>BP</sup> or Ga-NO2AP<sup>BP</sup> etc. are used for the ligands/complexes regardless of the in charge/protonation state, except when the distinction is necessary for comprehension.

This paper describes the synthesis of the ligands, their physicochemical characterization, the labeling with <sup>68</sup>Ga, the *in vitro* binding to HAP, the *ex-vivo* biodistribution of the <sup>68</sup>Ga-labeled compounds and small animal *in vivo* PET imaging.

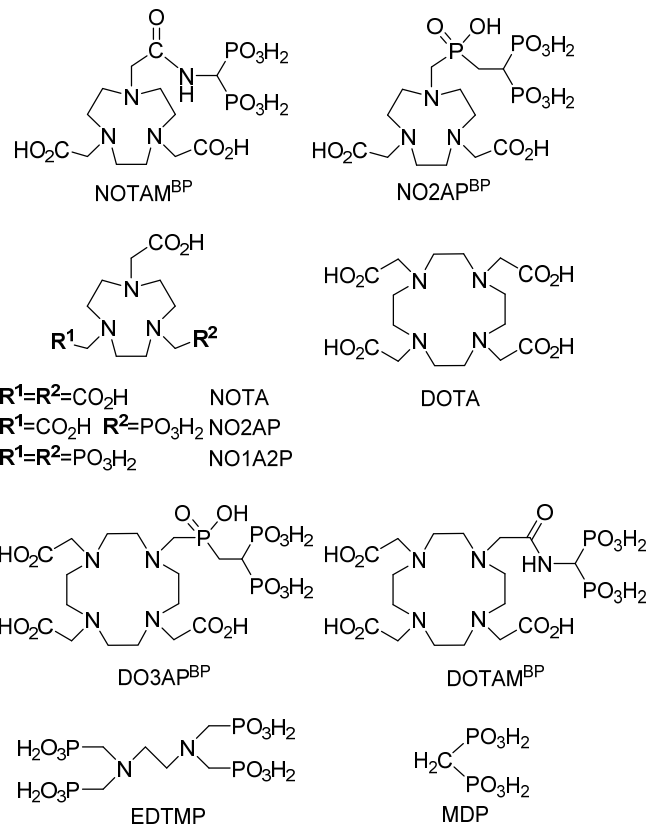


Fig. 1 Ligands discussed in this paper.

## Results and Discussion

### Synthesis

The ligands were synthesized according to Scheme 1. A previously described procedure<sup>23</sup> for the benzyl monoprotected macrocycle **2** was modified to a one-pot synthesis and its overall yield was improved. Further reaction with t-butyl bromoacetate followed by catalytic hydrogenation resulted in doubly substituted macrocycle **4**. Preparations of compound **4**, commonly used for synthesis of 1,4,7-triazacyclononane-1,4-diacetic acid (NO2A) derivatives, have been known for a long time,<sup>24</sup> however, the present synthesis was slightly modified, run in much higher scale and resulted in overall yield comparable with the previous ones. The secondary amine of the NO2A diester **4** was used for attachment of geminal bis(phosphonate) moiety via the acetamide or methylphosphinate linkers. The reactions were carried out with the fully esterified reagents due to their better solubility in organic solvents and more efficient chromatographic purification of the intermediates. The acetamide derivative **6** was prepared by alkylation of **4** with the appropriate chloroacetamide **5**. The phosphinate derivative **8** was prepared by Mannich-type reaction using para-formaldehyde and the per(ethyl) bis(phosphono)-phosphinate **7**. Cleavage of the ester protecting groups was performed in two steps. First, t-butyl groups were cleaved by action of trifluoroacetic acid and, then, ethyl groups were removed by transesterification with trimethylbromosilane followed by silyl group removal with methanol. The final purification on cation exchange resin yielded NOTAM<sup>BP</sup> and NO2AP<sup>BP</sup> in zwitterionic form.

<sup>85</sup> [Inset Scheme 1 here](#)

## Ga<sup>3+</sup> complexation

Coordination ability of the title ligands toward Ga(III) was studied due to their intended applications for <sup>68</sup>Ga PET imaging. In addition, Fe(III) complexes were prepared as this ion shows similar properties (the same charge and similar ionic radius) as Ga(III) and, thus, can be considered as a surrogate differing just in spectral and magnetic properties.

Dissolving the ligand in a solution containing the equimolar amount of the metal ions leads to significant decrease in pH (pH drops to 1.4–2.0). Addition of strong hydroxide and increase of pH (pH > 2) leads to immediate formation of precipitates. The precipitates are dissolved upon further increase in pH (pH > 4). Most likely, such behavior could be ascribed to a complex formation mechanism involving several intermediates as it has been suggested for similar macrocyclic ligands.<sup>8,19,20</sup> The initial mixing of the reagents leads to immediate coordination of the metal ion to the bis(phosphonate) oxygen atoms and release of protons. It is known that bis(phosphonate) group is able to interact with trivalent metal ions even at very low pH<sup>25,26</sup> and, at pH < 2, the ligands bind the metal ion in a protonated form (with protons bound on macrocyclic amines as well as on the phosphonate groups) forming out-of-cage complexes. Such species have overall positive charge and are soluble in water. Increase of pH causes further deprotonation of the bis(phosphonate) group and formation of charge-neutral complexes with low solubility in water. Such solid out-of-cage intermediates are expected to be 3-D coordination polymers having metal ions bridged by phosphonate group(s), typical for phosphonate and bis(phosphonate) complexes.<sup>25,26</sup> Further pH increase results in dissolution of the precipitates and is associated with the ring amine deprotonation and formation of final in-cage macrocyclic complexes where the metal ion is coordinated with three ring nitrogen atoms and three oxygen atoms of carboxylate or acetamide/phosphinate pendants.<sup>20,27</sup> A similar mechanism involving phosphonate-coordinated out-of-cage intermediate has been previously postulated for complexation of lanthanide(III) ions with analogous DOTA-like bis(phosphonate)-bearing ligands as DO3AP<sup>BP</sup>.<sup>6,8</sup> Formation of the in-cage complexes was confirmed by <sup>71</sup>Ga NMR measurements. The Ga-NO2AP<sup>BP</sup> complex shows a rather broad signal at 158 ppm ( $\epsilon_{1/2}$  ~1300 Hz, Figure S1). The quadrupole moment of the <sup>71</sup>Ga nucleus leads to a signal broadening if Ga(III) ion is placed in a non-symmetrical coordination environment. The non-symmetrical charge distribution leads to an extremely broad signal of Ga-NOTAM<sup>BP</sup> complex centered at ~170 ppm ( $\epsilon_{1/2}$  = ~9700 Hz, Figure S1); <sup>71</sup>Ga NMR chemical shift of 166 ppm has been observed for other NOTA-monoamide gallium(III) complex.<sup>22</sup>

The time course of gallium(III) complexation with the ligand NO2AP<sup>BP</sup> was studied in details by <sup>71</sup>Ga and <sup>31</sup>P{<sup>1</sup>H} NMR. Coordination spheres of the out-of-cage intermediates are completely non-symmetrical and, thus, are “invisible” in the <sup>71</sup>Ga NMR spectra. Thus, formation of the in-cage complex was quantified using an external capillary standard. These experiments were performed with Ga:L 1:1 molar ratio, at pH 2 and 3 (1 M sodium chloroacetate buffer), pH 4 and 5 (1 M sodium acetate buffer). In the presence of the weakly coordinating buffers, the above mentioned precipitation of intermediates was not observed. The results are summarized in

Table 1 and Figures 2 and S2. The complexation rates follow the order pH 2 < pH 3 ~ pH 5 < pH 4. As stated above, the complexation can be described as a two-step process. The intermediate out-of-cage complex is formed instantly and the metal ion is coordinated only through oxygen atoms of the bis(phosphonate) group and the pendant arms (carboxylate and phosphinate), whereas the macrocyclic amines are protonated. In the rate-determining step, the ring nitrogen atoms lost proton(s) and the metal ion simultaneously moves into the macrocycle cavity; it is, generally, a base-catalyzed process. The mechanism explains the increase in the complexation rate between pH 2 and 3. The slower complexation at pH 5 is probably caused by deprotonation of the bis(phosphonate) moiety leading to its stronger interaction with the Ga(III) ion and stabilization of the out-of-cage complex, or by formation of Ga(III) hydroxido complexes.

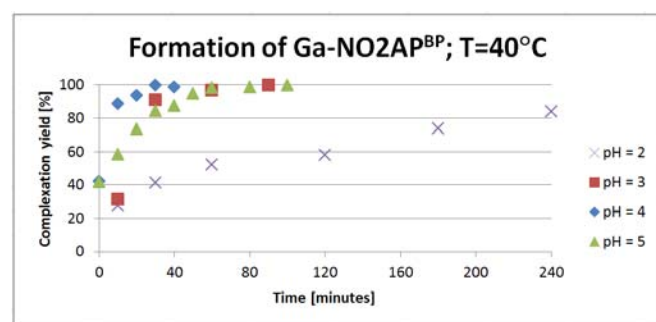


**Fig. 2** Time course of complexation of Ga(III) with NO2AP<sup>BP</sup> at 40 °C (molar ratio L : Ga = 1 : 1,  $c_{\text{Ga}} = 0.13$  M); dead time for  $t_0 = 5$  min.

**Table 1** Half-time ( $t_{1/2}$ ) of the Ga-NO2AP<sup>BP</sup> complex formation (40 °C, molar ratio L : Ga = 1 : 1,  $c_{\text{Ga}} = 0.13$  M).

| Ligand              | pH | $t_{1/2}$ [min] | 95 % complexation [min] |
|---------------------|----|-----------------|-------------------------|
| NO2AP <sup>BP</sup> | 5  | 10              | 50                      |
|                     | 4  | <5              | 20                      |
|                     | 3  | 12              | 60                      |
|                     | 2  | 65              | 360                     |
| NOTA <sup>a</sup>   | 3  | <2              |                         |
|                     | 1  | 270             |                         |

<sup>a</sup>25 °C, ref.<sup>19</sup>

In the case of NOTAM<sup>BP</sup>, the broadening of the <sup>71</sup>Ga NMR signal and overlapping of <sup>31</sup>P{<sup>1</sup>H} NMR signals of the product and reaction intermediates disabled precise quantification under the same conditions as those used for the NO2AP<sup>BP</sup> complexation. However, even after heating at 40 °C for several hours, broad <sup>31</sup>P{<sup>1</sup>H} NMR signals were observed showing that only an out-of-cage complex was formed, which was stable under these conditions. If the solution was heated at 95 °C (Figures 3 and S3), several signals could be distinguished after several minutes and the spectra indicate that the in-cage complex is fully formed after ~30 min under this conditions. Further heating led only to a decrease of the Ga-NOTAM<sup>BP</sup> complex signal and increase of that of the aminomethylene-bis(phosphonate) indicating that the Ga-NOTAM<sup>BP</sup> complex is unstable under this conditions and decomposes to the Ga-NOTA complex (see also below). Some decomposition (i.e. the formation of [Ga(NOTA)]) was observed in the <sup>71</sup>Ga NMR spectrum even after 10 min of the reaction (Figure S3).

The results point to an important role of the spacer connecting

the bis(phosphonate) group and the macrocycle. Under all conditions tested, NO2AP<sup>BP</sup> showed significantly faster gallium(III) complexation than NOTAM<sup>BP</sup>. Albeit phosphinates are known to be better complexation groups than carboxamides, the pronounced difference in the reaction rate is surprising. The hard phosphinate group as good coordinating group for Ga(III) ion is probably able to assist the ion transfer from the *out-of-cage* species into the *in-cage* complex much better than the carboxamide group does. In addition, basicity of the amine group in the >N-CH<sub>2</sub>-P(R)O<sub>2</sub>H moiety is significantly lowered<sup>19,28</sup> facilitating deprotonation of the adjacent amine group.

For both ligands, the complexation rates are significantly lower than those reported for NOTA or its phosphinic acid analogues.<sup>19,20,29</sup> So, presence of a too strongly complexing hard group such as the bis(phosphonate) one in the proximity of macrocycle could be considered as a rate-decreasing factor in Ga<sup>3+</sup> complexation reaction. In addition, it has been recently published that presence of three bis(phosphonate) groups in the side chains of a tris(methylenephosphinic acid) NOTA analog completely prevents entering the Ga(III) ion into the macrocyclic cavity and Ga(III) is coordinated only by the phosphonate groups in the *out-of-cage* fashion.<sup>30</sup> Consequently, a number of bis(phosphonate) groups should be balanced to have good bone targeting and, in the same time, efficient *in-cage* complexation.

#### Hydrolysis of the amide bond in the Ga-NOTAM<sup>BP</sup> complex

Single-crystals were formed in time course of Ga(III) complexation with NOTAM<sup>BP</sup>. According to the X-ray diffraction, these were not crystals of Ga-NOTAM<sup>BP</sup> but those of the known Ga-NOTA complex.<sup>27a</sup> It is result of the amide bond hydrolysis in the Ga-NOTAM<sup>BP</sup> complex (see also Figure 3). Upon complexation, Ga(III) is coordinated through amide oxygen or nitrogen atoms.<sup>21b</sup> This coordination decreases the electron density on the amide carbon atom and makes it more vulnerable for the solvent nucleophilic attack. (It is the same effect as expressed during hydrolysis of peptide bond catalyzed by metalloenzymes.)

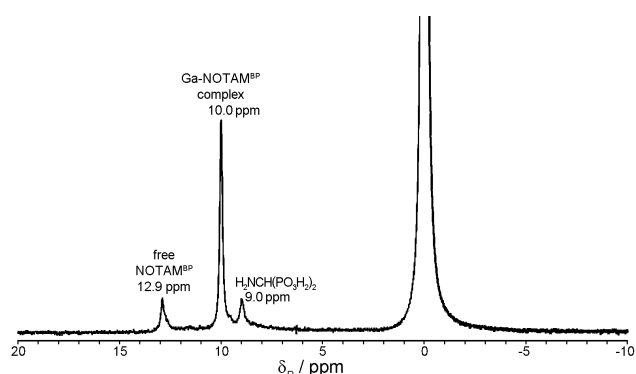


**Fig. 3** <sup>31</sup>P{<sup>1</sup>H} NMR spectrum of the reaction mixture after 30 min of reaction of Ga(III) with NOTAM<sup>BP</sup> at pH 3 and 90 °C (*c*<sub>Ga</sub> = 0.13 M, slight molar excess of the ligand; dead time (*t*<sub>0</sub>) approx. 5 min).

As the reaction is important in view of utilization of the <sup>68</sup>Ga-labelled ligands in nuclear medicine (see below), the hydrolysis was studied in more detail. It was monitored through an increasing intensity of the sharp Ga-NOTA signal in <sup>71</sup>Ga NMR (\*<sub>Ga</sub> = 170 ppm;  $\nu_{1/2}$  = 390 Hz) and, in parallel, through increasing intensity of the aminomethyl-bis(phosphonate) signal in <sup>31</sup>P{<sup>1</sup>H}

NMR ( $\Pi$  = 8.9 ppm, pH 3), Figure S3. The results show that the hydrolysis is faster with increasing pH (Figures 4). It indicates a hydroxide-mediated reaction and could be explained as nucleophilic attack of the hydroxide anion on the amide carbon atom. However, the hydrolysis proceeds with much slower rate than the formation of the *in-cage* complex as only very minor decomposition was observed during 10 min at 90 °C (Figure S3, see also above). The <sup>68</sup>Ga-NOTA complex as the hydrolysis product was not identified during the labeling with <sup>68</sup>Ga via radio-HPLC (see below). It should be noticed that analogous hydrolysis might have been present during studies of Ga(III) complexes with simple NOTA-monoamides where a very broad <sup>71</sup>Ga NMR signal of the complexes with a small sharp singlet at 170 ppm (probably attributable to the Ga-NOTA complex) was observed.<sup>21b</sup>

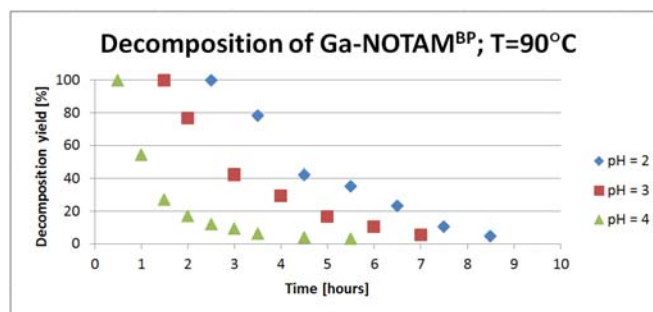
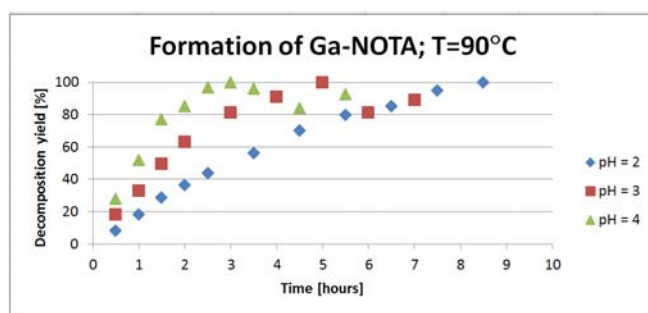


**Fig. 4** Hydrolysis of amide bond in the Ga-NOTAM<sup>BP</sup> complex expressed as increasing abundance of the Ga-NOTA complex in <sup>71</sup>Ga NMR and decreasing abundance of the Ga-NOTAM<sup>BP</sup> complex in <sup>31</sup>P{<sup>1</sup>H} NMR (90 °C, *c*<sub>Ga</sub> = 0.13 M). Figures do not have the same y-axis absolute scale: precipitation of the Ga-NOTA complex, confirmed by X-ray diffraction, caused decline of the <sup>71</sup>Ga NMR signal intensity by the end of the reaction and maximum in the <sup>31</sup>P{<sup>1</sup>H} NMR data refers to a time when the first integration was possible, i.e. after 0.5–2.5 h depending on pH.

#### Adsorption of iron(III) complexes on hydroxyapatite

To estimate bone targeting efficiency, the most commonly used method is to determine the binding ability of the molecules on hydroxyapatite (HAP) surface. For bis(phosphonate)-containing DOTA derivatives, the long-lived <sup>160</sup>Tb metal isotope has been used as a surrogate for lanthanide(III) ions.<sup>15</sup> As <sup>68</sup>Ga is a short-lived radioisotope, another method was sought. Trivalent iron has properties (charge, size, hardness etc.) similar to those of trivalent gallium and both ions form analogous complexes; thus, Fe(III) was chosen as a surrogate. UV-Vis spectroscopy was used to quantify the sorption ability as the Fe(III) complexes exhibit intensive LMCT band in UV region (Figure S4). The iron(III) complexes of DOTAM<sup>BP</sup> and DO3AP<sup>BP</sup> were also prepared and studied for comparison with analogous DOTA-like ligands already used as <sup>68</sup>Ga radiopharmaceuticals.<sup>13,14</sup>

The adsorption process is usually described by the Langmuir adsorption isotherm

$$\frac{X}{X_m} = \frac{K Z c}{1 + K Z c}$$

where  $K$  is the analyte (complex) affinity constant for surface (in  $\text{dm}^3 \text{mol}^{-1}$ ),  $X_m$  is the maximum sorption capacity of the complex (in  $\text{mol m}^{-2}$ ),  $c$  is the solution complex concentration (in  $\text{mol dm}^{-3}$ ) and  $X$  is the specific adsorbed amount of the complex (in  $\text{mol m}^{-2}$ ). Aqueous suspension of HAP was used as a model of bone tissue. The results are shown in Figure S5 and the adsorption parameters are summarized in Table 2.

**Table 2** Adsorption parameters of the Fe(III) complexes studied on hydroxyapatite surface (pH 7.5, 25 °C, equilibration time 3 d).

| Complex   | Fe-NOTAM <sup>BP</sup> | Fe-NO2AP <sup>BP</sup> | Fe-DOTAM <sup>BP</sup> | Fe-DO3AP <sup>BP</sup> |
|---|------------------------|------------------------|------------------------|------------------------|
| $K / 10^3$<br>( $\text{dm}^3 \text{mol}^{-1}$ ) | $31.3 \pm 6.1$         | $20.0 \pm 3.2$         | $43.7 \pm 12.2$        | $207.6 \pm 45.3$       |
| $X_m / 10^{-6}$<br>( $\text{mol m}^{-2}$ )      | $1.007 \pm 0.035$      | $1.271 \pm 0.052$      | $0.768 \pm 0.019$      | $1.015 \pm 0.017$      |

All complexes studied show efficient binding on the HAP surface. Maximum sorption capacities are in the range that corresponds to the formation of monomolecular layer.<sup>6</sup> For the complexes of NOTA analogues, maximum sorption capacities are higher than those for the of DOTA complexes. This could be explained by the compact shape of the Fe(III) complexes with NOTA derivatives, where all pendant arms are coordinated.<sup>31</sup> A larger size of the cyclen ring and presence of one uncoordinated pendant arm in the complexes with DOTA-like ligands<sup>32</sup> result in a larger surface area occupied by one molecule of the DOTA complexes. Higher affinity constants found for the complexes with DOTA derivatives indicate, that the uncoordinated pendant arm might be involved in the interaction with the HAP surface. Generally, both affinity constants as well as sorption capacities are comparable to those previously reported for lanthanide(III) complexes with the same DOTA analogs, where all pendant arms are bound to the central metal ion (e.g.  $K = 250 \cdot 10^{-3} \text{ dm}^3 \text{ mol}^{-1}$  and  $X_m = 0.65 \cdot 10^6 \text{ mol m}^{-2}$  for the  $^{160}\text{Tb-DO3AP}^{\text{BP}}$  complex)<sup>15</sup> as well as to those for simple bis(phosphonates), e.g. for pamidronate ( $K = 44 \cdot 10^{-3} \text{ dm}^3 \text{ mol}^{-1}$  and  $X_m = 1.82 \cdot 10^6 \text{ mol m}^{-2}$ ).<sup>15</sup> It indirectly confirms similar accessibility of the distant bis(phosphonate) moiety for bone targeting in all the complexes.

### Radiolabeling with no-carrier-added $^{68}\text{Ga}$

If ligands are considered as potential radiopharmaceuticals, the efficiency of metal radionuclide incorporation is one of their most important properties and, thus, the title ligands were tested in labeling with NCA  $^{68}\text{Ga}$ . The ligand-to- $^{68}\text{Ga}$ (III) molar ratio was approximated in the order of  $10^4$  in all experiments (1 MBq  $^{68}\text{Ga}$  corresponds to  $\sim 0.01 \text{ pmol}$  of  $\text{Ga}(\text{III})$ ). The complexation was followed (see an example of the TLC plate in ESI, Figure S6) at various temperatures and solution acidities, and the results are summarized in Figures 5 and 6.

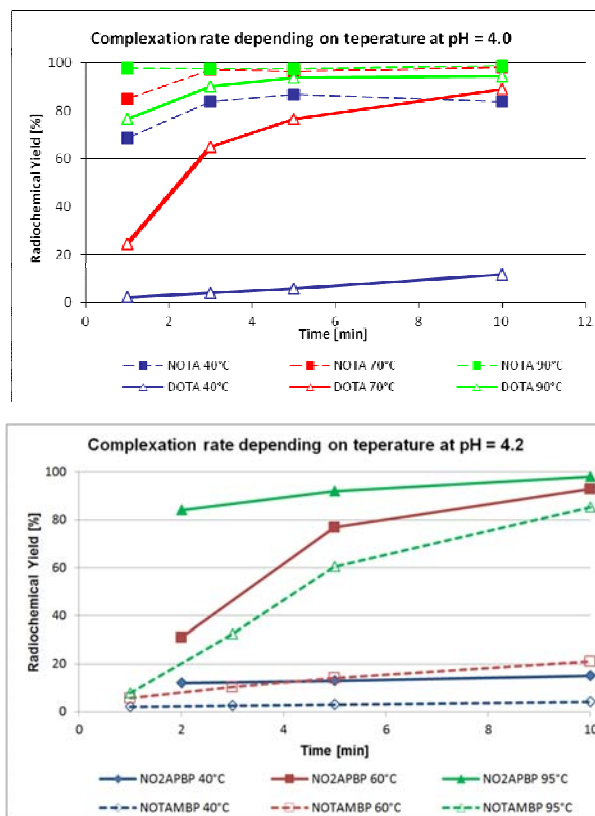


**Fig. 5** Time course of incorporation of no-carrier-added  $^{68}\text{Ga}(\text{III})$  by the title ligands at various temperatures.

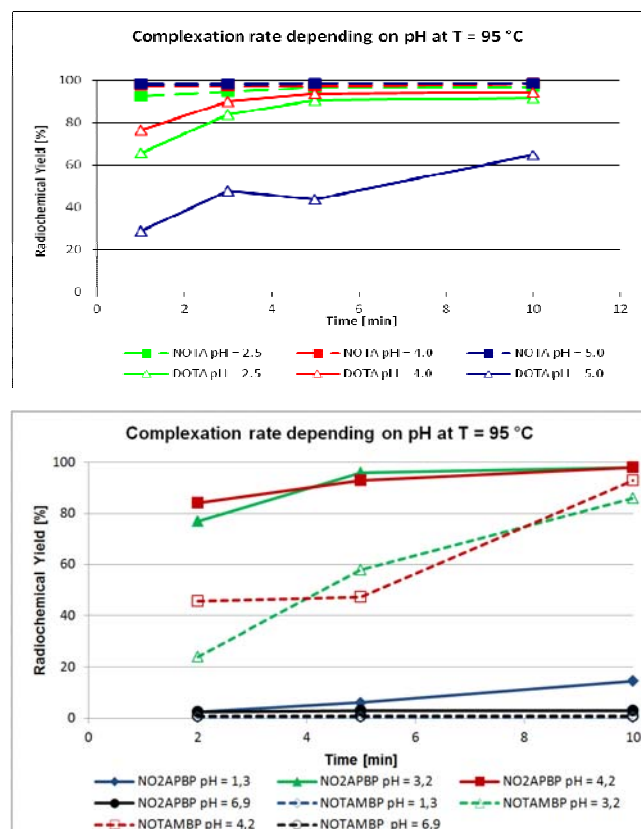


**Fig. 6** Time course of incorporation of no-carrier-added  $^{68}\text{Ga}(\text{III})$  by the title ligands at various pH.

The data show similar trends as those obtained in the NMR experiments (above). For both ligands, fast complexation requires weakly acidic conditions, i.e. pH 3–4. No complexation was observed at pH 1.3 and 6.9 at any temperature. The experiments also confirmed the strong dependence of the complexation rate on the temperature. At pH = 4.2 and at room temperature, no complexation was observed with both ligands. In the case of NO2AP<sup>BP</sup>, heating to 60 °C is required to reach full complexation in 10 min; at 95 °C <sup>68</sup>Ga(III) was quantitatively bound in only 5 min. Temperatures of <60 °C were insufficient for the radiolabeling with NOTAM<sup>BP</sup> and reasonable complexation efficiency was reached only at temperature of 95 °C. The amide bond hydrolysis was not observed during radiolabelling (radio-HPLC), mostly due to short labelling time. NO2AP<sup>BP</sup> shows much faster complexation of NCA <sup>68</sup>Ga(III) than NOTAM<sup>BP</sup> under all tested conditions (Figures 5 and 6). It has been shown (under the same conditions) that presence of one or two methylphosphonate arms in NOTA analogs (NO2AP and NO1A2P; for formulae, see Figure 1) accelerates the labeling reaction in comparison with the labeling with NOTA.<sup>33</sup> Thus, presence of methylenephosphonic/inic acid pendant arms seems to increase the complexation rate. Radiolabeling of the title ligands with NCA <sup>68</sup>Ga is less efficient than that of NOTA; however, NO2AP<sup>BP</sup> incorporates <sup>68</sup>Ga similarly to the unsubstituted DOTA (Figure 5 and 6). Both title ligands are more efficient chelators than DOTAM<sup>BP</sup> (it needs 20–25 min at 95 °C for 95 % labeling and the best pH is ~5; other labeling conditions are the same as for the title ligands).<sup>13</sup>

The <sup>68</sup>Ga-DOTAM<sup>BP</sup> complex have been already applied *in vivo*<sup>13,14</sup> and, compared to it, the <sup>68</sup>Ga-complexes of the title ligands appear better suited for straight forward labelling adequate to utilization *in vivo* (see below).

#### Adsorption of <sup>68</sup>Ga-labeled complexes to hydroxoapatite

Binding of complexes labeled with <sup>68</sup>Ga to HAP surface was measured at room temperature (Figure 7). The [<sup>68</sup>Ga]NO2AP<sup>BP</sup> complex (93.8±4.4 %) is bound much better compared to [<sup>68</sup>Ga]NOTAM<sup>BP</sup> complex (38.1±2.6 %), while binding of the [<sup>68</sup>Ga]NOTA complex (1.5±0.3 %) is negligible under the same conditions. These results are not fully paralleling those of iron(III) complexes obtained under “chemical” equilibrium conditions where no significant differences were observed. Because of the short half-life of <sup>68</sup>Ga, a short contact time of the complexes with HAP was used and full equilibrium could not be reached, unlike during measurements with the Fe(III) complexes (above). Thus, the difference between the experiments might be attributed to the faster absorption kinetics of [<sup>68</sup>Ga]NO2AP<sup>BP</sup> complex if compared with [<sup>68</sup>Ga]NOTAM<sup>BP</sup> complex; it was observed that the [<sup>160</sup>Tb]DO3AP<sup>BP</sup> complex adsorbs on HAP surface very quickly.<sup>16</sup> These results are more relevant for *in vivo* conditions. Compounds with low adsorption kinetics are not suitable for future *in vivo* studies. It is necessary to obtain high binding to the targeted tissue for imaging agents in a short timescale, otherwise long measurement time and high activities are required to develop adequate PET images. [<sup>68</sup>Ga]NO2AP<sup>BP</sup> had a binding of 93.8 ± 4.4 % on HAP after 10 min, which is one of the highest rates among <sup>68</sup>Ga-labelled bis(phosphonates) (Figure 7). The data in this experiment are well correlating with those of the bone accumulation *in vivo* (in *ex vivo* organ distribution, see below).

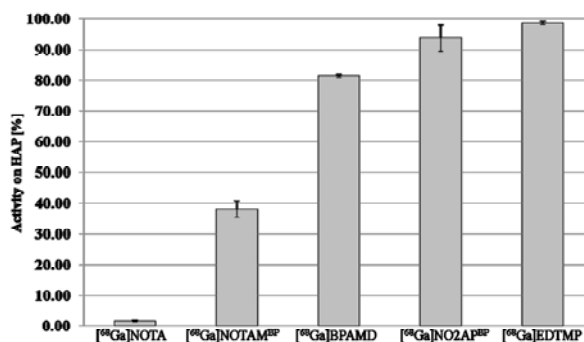


Fig. 7 Binding of <sup>68</sup>Ga-labeled complexes to hydroxoapatite in isotonic saline (room temperature, 10 min). Data for [<sup>68</sup>Ga]EDTMP<sup>33</sup> (for EDTMP formula, see Figure 1) and [<sup>68</sup>Ga]DOTAM<sup>BP</sup> (ref.<sup>13</sup>) are taken from literature.

#### *In vivo* biodistribution studies

Uptake in the bone was observed within few minutes as monitored via PET and the labeled compound were cleared out of the blood during 60–120 min via the kidneys and bladder. Similar results were observed with of [<sup>68</sup>Ga]DOTA-based bis(phosphonates) in already published data.<sup>13,34</sup> The data clearly shows high uptake of [<sup>68</sup>Ga]NO2AP<sup>BP</sup> in bone (femur 4.37 %, 60 min p.i.; Table 3) and very low uptake in not-target organs like soft tissues (Table 3). The bone uptake is superior if compared with the established PET bone tracer, [<sup>18</sup>F]NaF, and also higher than that of DOTA-based tracer (Figure 8). Lower uptake of [<sup>68</sup>Ga]NOTAM<sup>BP</sup> is in line with the *in vitro* results (above).

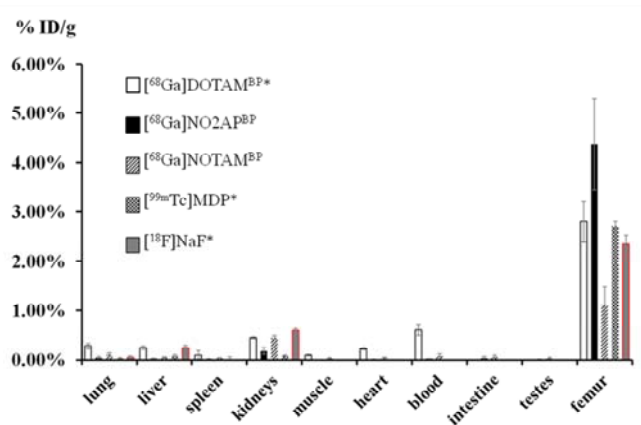


Fig. 8 Biodistribution data for different bone-binding <sup>68</sup>Ga radiotracers in healthy male Wistar rats (n = 5) after 60 min. p.i. \*Data for [<sup>68</sup>Ga]DOTAM<sup>BP</sup>, [<sup>18</sup>F]NaF<sup>34</sup> and [<sup>99m</sup>Tc]MDP<sup>34</sup> (for MDP formula, see Figure 1) are taken from literature.

Insert Table 3 here  
Insert Figure 9 here

The  $\mu$ PET images show a fast clearance of the compound out of the blood. After 5–10 min, only 10–15 % of the injected radiotracer is found in the bloodstream, while a very fast accumulation in the skeleton was observed. Bone images of good quality can be developed at early time points. In Figures 9 and S7, the skeleton is clearly highlighted after only 15 min. In the second animal (Figure 9), the kidneys show a high uptake as the

main clearance organ of the [<sup>68</sup>Ga]NO<sub>2</sub>AP<sup>BP</sup> as expressed by SUV (Standardized Uptake Value) in Figures S8 and S9. After a fast initial accumulation (up to 50 min. p.i.), the labeled compound is predominantly cleared to the bladder and washed out of the animal *via* the urine. [<sup>68</sup>Ga]NO<sub>2</sub>AP<sup>BP</sup> showed a similar kinetics in both animals with only small differences which could be explained by variation between the animals weight and age. At 60 min after p.i., the SUV in the spine was 1.8 for animal no. 1 (536 g, 32 MBq) and 1.6 for animal no. 2 (346 g, 31 MBq). Uptake of the <sup>68</sup>Ga-bis(phosphonate) in bone joints was almost 50 % higher (animal no. 1, SUV in the joint of the scapula and the humerus was 3.1).

## Conclusions

The new bis(phosphonate)-containing derivatives of NOTA were prepared by scaleable synthesis. They show efficient complexation of trivalent gallium, The phosphinate derivative was shown to bind the metal ion better than the acetamide derivative under any conditions used. The complexation rates of these new ligands were slower than those of NOTA or its phosphinic acid analogues due to presence of phosphonate groups forming rather stable *out-of-cage* complex which is able to compete with formation of the *in-cage* complex. The amide group in the *in-cage* complex is not fully hydrolytically stable due to a strong polarizing effect of the small Ga<sup>3+</sup> ion after its coordination; These results indicate that complexes of NOTA-amides can be hydrolytically unstable unlike complexes of DOTA-amides where analogous hydrolysis has not been observed; it should be taken into account while designing new ligands for Ga(III) and other highly charged metal ions. However, the hydrolysis takes place only at high temperature and is slow in comparison with the labeling time necessary for NCA <sup>68</sup>Ga. Radiolabeling with <sup>68</sup>Ga was fast at temperatures above 60 °C for the phosphinate and at 90 °C for the acetamide ligand. Biodistribution and μPET studies in healthy male rats showed very quick uptake of the <sup>68</sup>Ga-labeled probes on bones and fast elimination of the non-targeted probes through the kidneys. The pharmacokinetics of the new labeled macrocyclic ligands is similar to that of the labeled DOTA-bis(phosphonate) conjugates as well as that of commonly used <sup>99m</sup>Tc-bis(phosphonate) radiopharmaceuticals or [<sup>18</sup>F]Na, but results in a significantly higher accumulation of [<sup>68</sup>Ga]NO<sub>2</sub>AP<sup>BP</sup> (4.37±0.92 %ID/g) in the femur. These properties, together with the easy labeling process and the convenient availability of <sup>68</sup>Ga from commercial generators, render the title ligands, mainly the phosphinate derivative, as the best leading compounds for development of bone-targeted PET probes. Experiments focused on better understanding of biological fate and, finally, directed to a human application of the new probes are under way.

## Acknowledgement

Support from the Grant Agency of the Czech Republic (13-08336S), the Grant Agency of the Charles University in Prague (No. 19310) and the Long-Term Research Plan of the Ministry of Education of the Czech Republic (No. MSM0021620857) is acknowledged. The work was carried out in the framework of COST TD1004, TD1007 and CM0807 (PhoSciNet) Actions. We

are grateful to Nicole Bausbacher and Barbara Biesalski (Mainz University) for performing the animal experiments.

## Notes and references

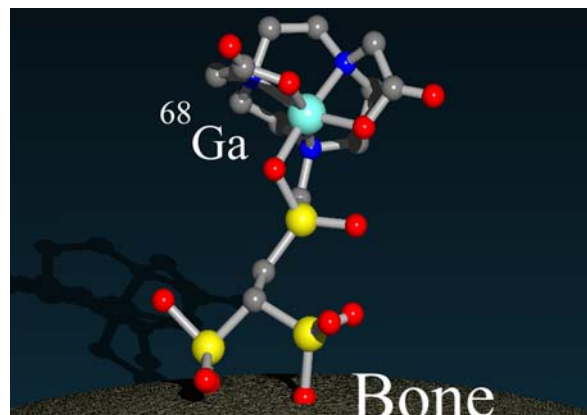
- <sup>a</sup> Department of Inorganic Chemistry, Faculty of Science, Charles University in Prague, Hlavova 2030, 128 43 Prague 2, Czech Republic. Fax: +420 22195 1253; Tel: +420 22195 1263; E-mail: [petrh@natur.cuni.cz](mailto:petrh@natur.cuni.cz)
- <sup>b</sup> Institute of Nuclear Chemistry, University Mainz, Fritz-Strassmann-Weg 2, 55128 Mainz, Germany.
- <sup>†</sup> Electronic Supplementary Information (ESI) available: <sup>31</sup>P and <sup>71</sup>Ga NMR spectra of complexes, time courses of complexation reactions followed by NMR spectroscopy, UV-VIS spectra of Fe(III) complexes, TLC evaluation of labeling with NCA <sup>68</sup>Ga, additional μPET image, SUV data, complete experimental details. See DOI: 10.1039/b000000x/
- (a) F. Roesch and P. J. Riss, *Curr. Top. Med. Chem.* 2010, **10**, 1633–1668. (b) M. Fani, J. P. André and H. R. Mäcke, *Contrast Media Mol. Imaging* 2008, **3**, 67–77; (c) T. J. Wadas, E. H. Wong, G. R. Weisman and C. J. Anderson, *Chem. Rev.* 2010, **110**, 2858–2902; (d) I. Velikyan, *Med. Chem.* 2011, **7**, 345–372; (e) W. A. P. Breeman, E. de Blois, H. S. Chan, M. Konijnenberg, D. J. Kwekkeboom and E. P. Krenning, *Semin. Nucl. Med.* 2011, **41**, 314–321; (f) M. D. Bartholomae, *Inorg. Chim. Acta* 2012, **389**, 36–51.
  - S. Zhang, G. Gangal and H. Uludag, *Chem. Soc. Rev.*, 2007, **36**, 507–531.
  - V. Kubiček and I. Lukeš, *Future Med. Chem.*, 2010, **2**, 521–531.
  - E. Palma, J. D. G. Correia, M. P. C. Campello and I. Santos, *Mol. Biosyst.*, 2011, **7**, 2950–2966.
  - H. Fleisch, *Bisphosphonates in Bone Disease*, 4<sup>th</sup> Ed., Academic Press, London 2000.
  - V. Kubiček, J. Rudovský, J. Kotek, P. Hermann, L. V. Elst, R. N. Muller, Z. I. Kolar, H. T. Wolterbeek, J. A. Peters and I. Lukeš, *J. Am. Chem. Soc.*, 2005, **127**, 16477–16485.
  - T. Vitha, V. Kubiček, P. Hermann, L. V. Elst, R. N. Muller, Z. I. Kolar, H. T. Wolterbeek, W. A. P. Breeman, I. Lukeš and J. A. Peters, *J. Med. Chem.*, 2008, **51**, 677–683.
  - T. Vitha, V. Kubiček, J. Kotek, P. Hermann, L. V. Elst, R. N. Muller, I. Lukeš and J. A. Peters, *Dalton Trans.*, 2009, 3204–3214.
  - W. Liu, A. Hajibeigi, M. Lin, C. L. Rostollan, Z. Kovács, O. K. Öz and X. Sun, *Bioorg. Med. Chem. Lett.*, 2008, **18**, 4789–4793.
  - K. Ogawa, H. Kawashima, K. Shiba, K. Washiyama, M. Yoshimoto, Y. Kiyono, M. Ueda, H. Mori and H. Saji, *Nucl. Med. Biol.*, 2009, **36**, 129–135.
  - K. Suzuki, M. Satake, J. Suwada, S. Oshikiri, H. Ashino, H. Dozono, A. Hino, H. Kasahara and T. Minamizawa, *Nucl. Med. Biol.*, 2011, **38**, 1011–1018.
  - M. Fellner, R. P. Baum, V. Kubiček, P. Hermann, I. Lukeš, V. Prasat and F. Rösch, *Eur. J. Nucl. Med. Mol. Imaging*, 2010, **37**, 834.
  - M. Fellner, B. Biesalski, N. Bausbacher, V. Kubiček, P. Hermann, F. Rösch and O. Thews, *Nucl. Med. Biol.*, 2012, **39**, 993–996.
  - R. P. Baum and H. R. Kulkarni, *Theranostics*, 2012, **2**, 437–447.
  - T. Vitha, V. Kubiček, P. Hermann, Z. I. Kolar, H. T. Wolterbeek, J. A. Peters and I. Lukeš, *Langmuir*, 2008, **24**, 1952–1958.
  - C. Rill, Z. I. Kolar, G. Kickelbick, H. T. Wolterbeek and J. A. Peters, *Langmuir*, 2009, **25**, 2294–2301.
  - (a) A. Heppeler, S. Froidevaux, H. R. Mäcke, E. Jermann, M. Béhé, P. Powell and M. Hennig, *Chem. Eur. J.*, 1999, **5**, 1974–1981; (b) W. Niu, E. H. Wong, G. R. Weisman, Y. Peng, C. J. Anderson, L. N. Zakharov, J. A. Golen and A. L. Rheingold, *Eur. J. Inorg. Chem.*, 2004, 3310–3315; (c) N. A. Cola, R. S. Rarig, Jr., W. Ouellette and R. P. Doyle, *Polyhedron*, 2006, **25**, 3457–3462; (d) C.-T. Yang, Y. Li and S. Liu, *Inorg. Chem.*, 2007, **46**, 8988–8997.
  - V. Kubiček, J. Havlíčková, J. Kotek, G. Tircsó, P. Hermann, É. Tóth and I. Lukeš, *Inorg. Chem.*, 2010, **49**, 10960–10969.
  - J. Šimeček, M. Schulz, J. Notni, J. Plutnar, V. Kubiček, J. Havlíčková and P. Hermann, *Inorg. Chem.*, 2012, **51**, 577–590.

- 20 J. Notni, P. Hermann, J. Havlíčková, J. Kotek, V. Kubiček, J. Plutnar, N. Loktionova, P. J. Riss, F. Rösch and I. Lukeš, *Chem. Eur. J.*, 2010, **16**, 7174–7185.
- 21 (a) D. Shetty, J. M. Jeong, C. H. Ju, Y. J. Kim, J.-Y. Lee, Y.-S. Lee, D. S. Lee, J.-K. Chung and M. C. Lee, *Bioorg. Med. Chem.*, 2010, **18**, 7338–7347; (b) D. Shetty, S. Y. Choi, J. M. Jeong, L. Hoigebazar, Y.-S. Lee, D. S. Lee, J.-K. Chung, M. C. Lee and Y. K. Chung, *Eur. J. Inorg. Chem.*, 2010, 5432–5438; (c) L. Hoigebazar, J. M. Jeong, S. Y. Choi, J. Y. Choi, D. Shetty, Y.-S. Lee, D. S. Lee, J.-K. Chung, M. C. Lee and Y. K. Chung, *J. Med. Chem.*, 2010, **53**, 6378–6385.
- 22 A. de Sá, Á. A. Matias, M. I. M. Prata, C. F. G. C. Geraldes, P. M. T. Ferreira and J. P. André, *Bioorg. Med. Chem. Lett.*, 2010, **20**, 7345–7348.
- 23 A. J. Blake, I. A. Fallis, R. O. Gould, S. Persons, S. A. Ross and M. Schröder, *J. Chem. Soc., Dalton Trans.*, 1996, 4379–4387.
- 24 (a) J. Huskens and A. D. Sherry, *J. Am. Chem. Soc.*, 1996, **118**, 4396–404; (b) H.-S. Chong, H. A. Song, N. Birch, T. Le, S. Lim and X. Ma, *Bioorg. Med. Chem. Lett.*, 2008, **18**, 3436–3439; (c) P. J. Riss, C. Kroll, V. Nagel and F. Rösch, *Bioorg. Med. Chem. Lett.*, 2008, **18**, 5364–5367; (d) D. Shetty, S. Y. Choi, J. M. Jeong, J. Y. Lee, L. Hoigebazar, Y.-S. Lee, D. S. Lee, J.-K. Chung, M. C. Lee and Y. K. Chung, *Chem. Commun.*, 2011, **47**, 9732–9734.
- 25 E. Matczak-Jon and V. Videnova-Adrabinska, *Coord. Chem. Rev.*, 2005, **249**, 2458–2488.
- 26 V. Kubiček, J. Kotek, P. Hermann and I. Lukeš, *Eur. J. Inorg. Chem.*, 2007, 333–344.
- 27 (a) C. Broan, J. P. Cox, A. S. Craig, R. Katakya, D. Parker, A. Harrison, A. M. Randall and G. Ferguson, *J. Chem. Soc., Perkin Trans. 2*, 1991, 87–99; (b) J. P. André, H. R. Mäcke, M. Zehnder, L. Macko and K. G. Akyel, *Chem. Commun.*, 1998, 1301–1302.
- 28 I. Lukeš, J. Kotek, P. Vojtišek and P. Hermann, *Coord. Chem. Rev.*, 2001, **216&217**, 287–312.
- 29 (a) J. Notni, J. Šimeček, P. Hermann, K. Pohle and H.-J. Wester, *Chem. Eur. J.*, 2011, **17**, 14718–14722; (b) J. Šimeček, J. Notni, O. Zemek, P. Hermann and H.-J. Wester, *ChemMedChem*, 2012, **7**, 1375–1378. (c) J. Šimeček, P. Hermann, H.-J. Wester and J. Notni, *ChemMedChem*, 2013, **8**, 95–103
- 30 J. Notni, J. Plutnar and H.-J. Wester, *EJNMMI Res.*, 2012, **2**, 13.
- 31 (a) K. Wiegardt, U. Bossek, P. Chaudhuri, W. Herrmann, B. C. Menke and J. Weiss, *Inorg. Chem.*, 1982, **21**, 4308–4314; (b) D. A. Dixon, M. Shang and A. G. Lappin, *Inorg. Chim. Acta*, 1999, **290**, 197–206.
- 32 C. A. Chang, L. C. Francesconi, M. F. Malley, K. Kumar, J. Z. Gougoutas and M. F. Tweedle, *Inorg. Chem.*, 1993, **32**, 3501–3508.
- 33 M. Fellner, P. Riss, N. Loktionova, K. Zhernosekov, O. Thews, C. F. G. C. Geraldes, Z. Kovács, I. Lukeš and F. Rösch, *Radiochim. Acta*, 2011, **99**, 43–51.
- 34 M. Meckel, M. Fellner, R. Bergmann and F. Rösch, *Nucl. Med. Biol.* 2013, accepted.

70

## Table of Contents

NOTA monophosphinate and monocarboxamide analogs with bis(phosphonate) side group in the pendant arm were efficiently labeled with  $^{68}\text{Ga}$  and complex of the phosphinate-bis(phosphonate) ligand exhibit very high affinity for hydroxoapatite *in vitro* and bones *in vivo* and, thus, they are promising for effective PET imaging of bone metastases.



80

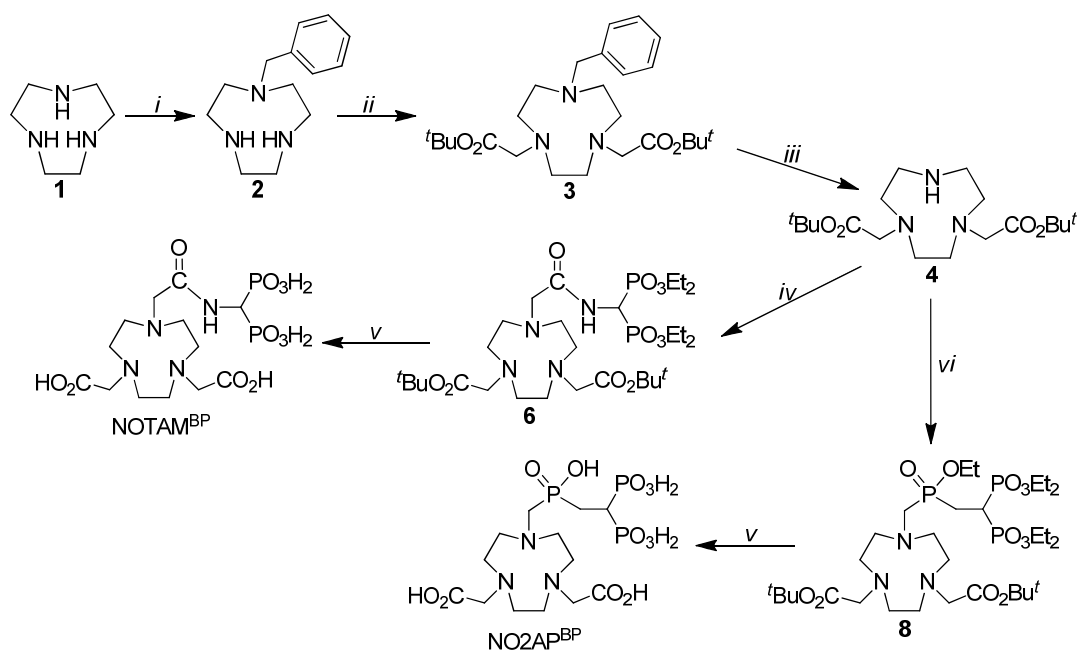
## Running Footer

Bis(phosphonate) NOTA analogs for PET bone imaging

55

60

65



**Scheme 1** Syntheses of ligands: (i) 1. Me<sub>2</sub>NCH(OMe)<sub>2</sub>, dioxan, reflux, 3 h; 2. BrCH<sub>2</sub>Ph, THF, r.t., overnight; 3. KOH, H<sub>2</sub>O/EtOH, reflux, 3 d; 75 %. (ii) BrCH<sub>2</sub>CO<sub>2</sub><sup>t</sup>Bu, K<sub>2</sub>CO<sub>3</sub>, acetonitrile, r.t., 3 d; 91 %. (iii) H<sub>2</sub>, Pd/C, EtOH, 50 °C, 12 h; 84 %. (iv) ClCH<sub>2</sub>C(O)NH-CH(PO<sub>3</sub>Et<sub>2</sub>)<sub>2</sub> (5), K<sub>2</sub>CO<sub>3</sub>, acetonitrile, 50 °C, 3 d; 83 %. (v) 1. CF<sub>3</sub>CO<sub>2</sub>H/CHCl<sub>3</sub> 1:1, r.t., 12 h; 2. BrSiMe<sub>3</sub>, acetonitrile, r.t., 12 h; 80 % (NOTAM<sup>BP</sup>), 41 % (NO2AP<sup>BP</sup>). (vi) HP(O)(OEt)CH<sub>2</sub>CH(PO<sub>3</sub>Et<sub>2</sub>)<sub>2</sub> (7), (CH<sub>2</sub>O)<sub>n</sub>, acetonitrile, 35 °C, 3 d; 72 %.

10

**Table 3** *Ex vivo* biodistribution of [<sup>68</sup>Ga]NOTAM<sup>BP</sup> and [<sup>68</sup>Ga]NO2AP<sup>BP</sup> complexes in healthy male Wistar rats (60 min p.i.). Data are presented as an average from five animals (χ S.D.); uptake as % I.D. per gram of tissue (% ID/g).

| Complex                                | Organ     |           |           |           |           |           |           |           |           |           |
|--|-----------|-----------|-----------|-----------|-----------|-----------|-----------|-----------|-----------|-----------|
|  | Lung      | Liver     | Spleen    | Kidney    | Muscle    | Heart     | Blood     | Intestine | Testes    | Femur     |
| [ <sup>68</sup> Ga]NOTAM <sup>BP</sup> | 0.1220.03 | 0.0520.01 | 0.0420.01 | 0.4520.04 | 0.0320.01 | 0.0420.01 | 0.0920.04 | 0.0720.03 | 0.0420.01 | 1.1230.36 |
| [ <sup>68</sup> Ga]NO2AP <sup>BP</sup> | 0.0420.03 | 0.0220.01 | 0.0220.01 | 0.1820.07 | 0.0120.00 | 0.0120.01 | 0.0220.00 | 0.0320.03 | 0.0120.00 | 4.3760.92 |

20

25

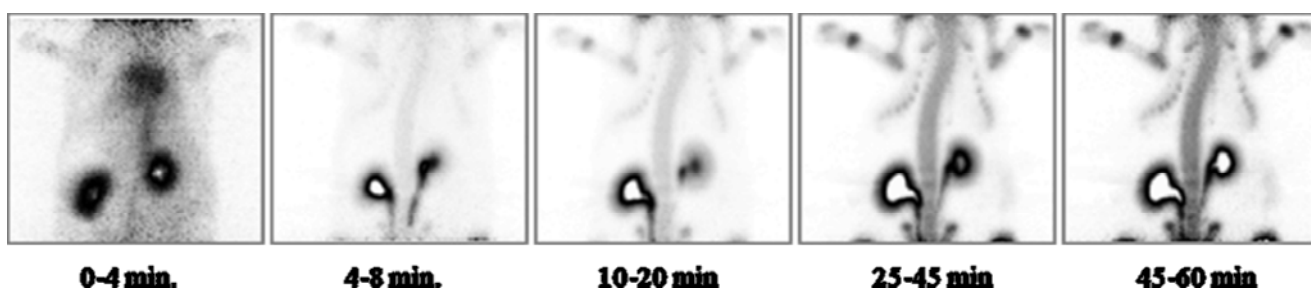


**Fig. 9** μPET image of the 2<sup>nd</sup> healthy male Wistar rat at different times after injection of 31 MBq [<sup>68</sup>Ga]NO2AP<sup>BP</sup>.

30